Large enhancement of thermoelectric effects in multiple quantum dots in a serial configuration due to Coulomb interactions

IOP Publishing Journal of Physics: Condensed Matter
J. Phys.: Condens. Matter **34** (2022) 255302 (7pp) https://doi.org/10.1088/1361-648X/ac640c

Large enhancement of thermoelectric effects in multiple quantum dots in a serial configuration due to Coulomb interactions

Natalya A Zimbovskaya*

Department of Physics and Electronics, University of Puerto Rico-Humacao, CUH Station, Humacao, PR 00791, United States of America

E-mail: natalya.zimbovskaya@upr.edu

Received 18 January 2022, revised 19 March 2022
Accepted for publication 4 April 2022
Published 20 April 2022

Abstract

In the present work we theoretically study Seebeck effect in a set of several quantum dots in a serial configuration coupled to nonmagnetic conducting electrodes. We focus on the combined effect of intra-dot Coulomb interactions between electrons and the number of dots on the thermopower (S) and the thermoelectric figure of merit (ZT) of the considered transport junction within the Coulomb blockade regime. We show that a strong enhancement of the both S and ZT may occur when the chemical potential of electrodes is situated within the Coulomb gap in the electron transmission spectrum thus indicating a possibility of significant increase of the efficiency of heat-to-electric energy conversion. The enhancement becomes more pronounced when the number of dots increases.

Keywords: thermoelectric, effects, multiple, quantum, dots

(Some figures may appear in colour only in the online journal)

1. Introduction

Thermoelectric transport through single/multiple quantum dots (QDs) and molecules sandwiched between conducting electrodes attracted a significant interest of the research community in the past two decades [1–4]. Alongside other potentially useful properties these systems hold promise for enhanced efficiency of heat-to-electric-energy conversion. Numerous works were focused on Seebeck effect in nanoscale transport junctions which is directly responsible for the energy conversion. The effect is measured by recording the voltage ΔV canceling a charge current driven by the temperature difference between the electrodes ΔT [5, 6]. When ΔT remains much smaller than the temperatures of the electrodes T_α ($\alpha = \{\mathrm{L}, \mathrm{R}\}$) the system operates within the linear response regime and $\Delta V = -S\Delta T$ where the thermopower (Seebeck coefficient) S does not depend on the temperature gradient. As the difference between the temperatures of electrodes increases, the system may switch to a nonlinear regime, and the thermopower becomes a function of ΔT. In the present work we restrict ourselves with the analysis of certain aspects of linear Seebeck effect.

It was established that thermoelectric properties of nanoscale transport junctions were controlled by several factors including the geometry of the linker, the specifics of its coupling to the electrodes [5–12] and interactions between traveling electrons and linker vibrations and/or environmental nuclear motions [13–19]. Furthermore, Seebeck coefficient may be affected by quantum interference effects [11, 17, 20–24] and by electron photon interactions [25, 26]. Under certain conditions (e.g. in the case of ferromagnetic electrodes), spin polarization of electrons may result in spin Seebeck effect [21, 27–33].

Thermoelectric transport through a long molecule made out of repeating units such as benzene or phenyl rings strongly depends on the number of these subunits which determines the molecular length [5–7, 9, 12, 34]. Similar dependencies may be expected for characteristics of electron transport through

* Author to whom any correspondence should be addressed.

a set of QDs arranged in a serial configuration [11]. Also it is well established that Coulomb interactions between electrons may affect characteristics of thermoelectric transport in nanoscale systems [20–23, 27, 32, 35–44]. For instance, it was shown that the thermal efficiency of a double QD coupled to the electrodes in a parallel configuration may be significantly enhanced due to intra-dot Coulomb interactions [20].

Models commonly employed to analyze the effects of electron–electron interactions on the electron transport through QDs/molecules usually simulate them either as single-level systems [7–9, 13, 22, 35–39, 42] or as double [20, 21, 32, 39, 41, 44] and triple [40] single-level dots in a parallel configuration. The same models could be applied to describe multilevel systems where each level is coupled to the electrodes [27]. Effects of electron–electron interactions on thermoelectric properties of a set of QDs in a serial configuration are less thoroughly studied so far. These effects were briefly analyzed together with quantum interference effects occurring when electrons tunnel through a chain compiled of several single-level QDs and supplemented with side dots providing for multiple pathways for traveling electrons [11]. Also, the influence of Coulomb interactions on characteristics of thermoelectric electron transport in a double dot wired in series within both linear and nonlinear transport regime was recently studied in reference [43].

In the present work we employ a simple tight-binding model of a transport junction including an arbitrary number of single-level QDs wired in series. In contrast to previous works [11, 20, 21, 27, 32, 39–41, 44] this model allows us to study the combined effect of the length of the chain compiled of QDs and Coulomb interactions between electrons on the characteristics of thermoelectric transport avoiding the influence of quantum interference. We show that in sufficiently long QD chains intra-dot Coulomb interactions could significantly modify characteristics of electron thermoelectric transport increasing the efficiency of heat-to-electric energy conversion.

Present results may not be considered as a simple generalization of those reported in reference [43] for they are obtained under different assumptions concerning Coulomb interactions. Here we concentrate on the effect of intra-dot Coulomb interactions neglecting weaker inter-dot electron–electron interactions whereas in the earlier work [43] the research was carried out in the limit of infinitely strong intra-dot electron–electron interactions and focused on the effect of inter-dot Coulomb interactions on the charge and heat current rectification. This difference prevents a straightforward comparison of the results obtained here for the case of a double dot wired in series with the corresponding results of reference [43].

2. Model and formalism

We consider a set of N single-level QDs arranged in series. An ith dot is assigned an on-site energy E_i and coupled to its nearest neighbors with coupling strengths $\beta_{i-1,i}$ and $\beta_{i,i+1}$ ($2 \leqslant i \leqslant N-1$), respectively. Terminal dots in the chain are supposed to be attached to nonmagnetic conducting electrodes. Similar models were used to mimic molecular bridges comprised of repeating units in metal–molecule junctions (see e.g. references [7, 34, 45]). Coulomb interactions between electrons on the same dot are characterized by charging energies U_i. We omit interdot Coulomb interactions which usually are much weaker than intra-dot ones. It is known that phonons may have a rather weak effect on electron transport through QDs and/or molecules (see e.g. references [46, 47]). On these grounds, electron–phonon interactions are often omitted when studies electron transport through these systems are carried on. In further analysis we also omit from consideration electron–phonon interactions and assume that coherent electron transmission is the predominating transport mechanism.

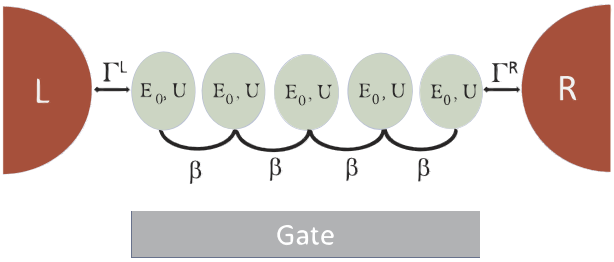

Figure 1. Schematics of the employed model. Several identical QDs with on-dot energies E_0 and intra-dot charging energies U are connected in series via the coupling parameter β and coupled to the electrodes via tunneling rates Γ^α, ($\alpha = \{\mathrm{L}, \mathrm{R}\}$).

To simplify the accepted model we suppose that all on-site energies E_i and charging energies U_i are equal ($E_i = E_0$, $U_i = U$) as well as coupling parameters ($\beta_{i-1,i} = \beta_{i,i+1} = \beta$). Schematics of the model is presented in figure 1. Within the chosen model the Hamiltonian of the considered system may be written in the form:

$$H = H_{\mathrm{E}} + H_d + H_t. \tag{1}$$

Here, H_{E} describes the electrodes:

$$H_{\mathrm{E}} = \sum_{\alpha,k,\sigma} \epsilon_{\alpha,k,\sigma} C^{\dagger}_{\alpha,k,\sigma} C_{\alpha,k,\sigma}, \tag{2}$$

where $\alpha = \{\mathrm{L}, \mathrm{R}\}$ labels the left and right electrodes, $\epsilon_{\alpha,k,\sigma}$ are single electron energies in the electrodes with the wave vectors $\mathbf{k}$ and spin σ and $C^{\dagger}_{\alpha,k,\sigma}, C_{\alpha,k,\sigma}$ are creation and annihilation operators for these electrons.

The term H_d is associated with the dots:

$$H_d = \sum_{i,\sigma} n_{i,\sigma}(E_0 + U n_{i,-\sigma}) + \beta \sum_{i,\sigma} \left(d^{\dagger}_{i,\sigma} \left[d_{i+1,\sigma}(1-\delta_{iN}) + d_{i-1,\sigma}(1-\delta_{i1}) \right] + \mathrm{H.C.} \right). \tag{3}$$

In this expression, $1 \leqslant i \leqslant N$, $d^{\dagger}_{i,\sigma}, d_{i,\sigma}$ are creation and annihilation operators for electrons on the ith dot, $n_{i,\sigma} = d^{\dagger}_{i,\sigma} d_{i,\sigma}$ is the particles number operator and δ_{ij} is the Kronecker symbol.

Assuming that the first ($i = 1$) and the last ($i = N$) dots are coupled to the left and right electrodes, respectively, the transfer Hamiltonian which describes spin conserving electron

tunneling through the system may be written as follows:

$$H_t = \sum_{k,\sigma}\left(V^*_{\mathrm{L},k,\sigma}C^\dagger_{\mathrm{L},k,\sigma}d_{1,\sigma} + V^*_{\mathrm{R},k,\sigma}C^\dagger_{\mathrm{R},k,\sigma}d_{N,\sigma} + \mathrm{H.C.}\right), \quad (4)$$

where $V_{\alpha,k,\sigma}$ represent the relevant coupling strengths. Tunneling rates between the terminal dots and electrodes are given by:

$$\Gamma^\alpha_\sigma(E) = 2\pi\sum_k |V_{\alpha,k\sigma}|^2\delta(E-\epsilon_{\alpha,k,\sigma}). \quad (5)$$

Further we use a wide band approximation treating the tunnel rates as constants. In a symmetrically coupled system with nonmagnetic electrodes these constants do not depend on spin orientation and are equal to each other: $\Gamma^\alpha_\sigma = \Gamma$.

Starting from the Hamiltonian (1) we may derive expressions for the retarded ($\mathbf{G}^r_\sigma(E)$) and advanced ($\mathbf{G}^a_\sigma(E)$) electron Green's functions for the considered multiple dot which are presented by $N\times N$ matrices. Since no spin flip processes are taken into account the Green's functions may be separately introduced for transport channels with different spin orientation. Expressions for matrix elements $G^r(E)_{ij,\sigma} = \langle\langle d_{i,\sigma}; d^\dagger_{j,\sigma}\rangle\rangle$ are computed using the equations of motion method in the form suggested in references [48, 49] within the Coulomb blockade regime where charging energies significantly exceed thermal energies kT_α (k being the Boltzmann constant) as well as the coupling strength of the terminal dots to electrodes Γ.

It could be shown that matrix elements $\langle\langle d_{i,\sigma}; d^\dagger_{j,\sigma}\rangle\rangle$ for $2\leqslant i\leqslant N-1$ and $1\leqslant j\leqslant N$ are determined by linear equations:

$$\langle\langle d_{i,\sigma}; d^\dagger_{j,\sigma}\rangle\rangle - \upsilon_{i,\sigma}\left(\langle\langle d_{i-1,\sigma}; d^\dagger_{j,\sigma}\rangle\rangle + \langle\langle d_{i+1,\sigma}; d^\dagger_{j,\sigma}\rangle\rangle\right) = \upsilon_{i,\sigma}\delta_{ij}, \quad (6)$$

whereas $\langle\langle d_{1,\sigma}; d^\dagger_{j,\sigma}\rangle\rangle$ and $\langle\langle d_{N,\sigma}; d^\dagger_{j,\sigma}\rangle\rangle$ are determined by equations:

$$\begin{aligned}\langle\langle d_{1,\sigma}; d^\dagger_{j,\sigma}\rangle\rangle - \upsilon_{1,\sigma}\langle\langle d_{2,\sigma}; d^\dagger_{j,\sigma}\rangle\rangle &= \upsilon_{1,\sigma}\delta_{1j};\\ \langle\langle d_{N,\sigma}; d^\dagger_{j,\sigma}\rangle\rangle - \upsilon_{N,\sigma}\langle\langle d_{N-1,\sigma}; d^\dagger_{j,\sigma}\rangle\rangle &= \upsilon_{N,\sigma}\delta_{Nj}.\end{aligned} \quad (7)$$

In deriving equations (6) and (7) we used the following approximation to decouple some four-operator averages: $\langle\langle A^\dagger BC;\ D^\dagger\rangle\rangle \approx \langle A^\dagger B\rangle\langle\langle C;\ D^\dagger\rangle\rangle - \langle A^\dagger C\rangle\langle\langle B;\ D^\dagger\rangle\rangle$ [50].

In these equations:

$$\begin{aligned}\upsilon_{1,\sigma}(E) &= \frac{\left(1-\langle n_{1,-\sigma}\rangle\right)}{E-E_0+i\Gamma} + \frac{\langle n_{1,-\sigma}\rangle}{E-E_0-U+i\Gamma};\\ \upsilon_{N,\sigma}(E) &= \frac{\left(1-\langle n_{N,-\sigma}\rangle\right)}{E-E_0+i\Gamma} + \frac{\langle n_{N,-\sigma}\rangle}{E-E_0-U+i\Gamma};\end{aligned} \quad (8)$$

and

$$\upsilon_{i,\sigma}(E) = \frac{\left(1-\langle n_{i,-\sigma}\rangle\right)}{E-E_0+i\eta} + \frac{\langle n_{i,-\sigma}\rangle}{E-E_0-U+i\eta}, \quad (9)$$

when $2\leqslant i\leqslant N-1$. Here, η is a positive infinitesimal parameter, and electron occupation numbers on the dots $\langle n_{i,\sigma}\rangle$ are given by:

$$\langle n_{i,\sigma}\rangle = \frac{1}{2\pi i}\int \mathrm{d}E\, G^<_{ii,\sigma}(E), \quad (10)$$

where the lesser Green's function $\mathbf{G}^<_\sigma(E)$ may be approximated as $\mathbf{G}^<_\sigma(E) = i\sum_\alpha f^\alpha_\sigma \mathbf{G}^r_\sigma(E)\mathbf{\Gamma}^\alpha_\sigma\mathbf{G}^a_\sigma(E)$, f^α_σ ($\alpha = \{\mathrm{L},\mathrm{R}\}$) being Fermi distribution functions for electrodes with chemical potentials $\mu_{\alpha,\sigma}$ and temperatures T_α. Note that in a nonmagnetic system Green's functions do not depend on the electron spin orientation, as well as transfer matrices $\mathbf{\Gamma}^\alpha_\sigma$. Accepting a serial configuration for the dots and symmetric coupling to the electrodes each $N\times N$ transfer matrix $\mathbf{\Gamma}^\alpha$ has a sole nonzero element, namely, $\Gamma^{\mathrm{L}}_{11} = \Gamma^{\mathrm{R}}_{NN} = \Gamma$.

We compute the Green's functions matrix elements by self-consistently solving equations (6)–(10). Then we can find the electron transmission function $\tau(E) = \mathrm{Tr}\{\mathbf{G}^a(E)\mathbf{\Gamma}^{\mathrm{R}}\mathbf{G}^r(E)\mathbf{\Gamma}^{\mathrm{L}}\}$ which controls transport characteristics. In the considered system the expression for the electron transmission is reduced to the form: $\tau(E) = \Gamma^2|G^r_{1N}|^2$ which is employed in further analysis.

In general, the difference between the electrodes temperatures may give rise to corrections to the on-site energies proportional to $k\Delta T$ making the Green's functions matrix elements temperature-dependent [7, 35], and this may bring noticeable changes into the electron transmission provided that the energies on the dots accept values comparable with the these corrections. However, below we assume that $E_0 \gg k\Delta T$, and the corrections become negligible.

3. Results and discussion

At low temperatures electron electrical conductance G, thermal conductance $\varkappa_{\mathrm{el}}$ and Seebeck coefficient S may be directly computed from the electron transmission $\tau(E)$ provided that the latter smoothly varies near $E=\mu$ (μ being the chemical potential of electrodes in the absence of thermal and electrical bias) and that the temperature difference between the electrodes ΔT is much smaller than $T = \frac{1}{2}(T_{\mathrm{L}}+T_{\mathrm{R}})$ thus ensuring the linear response regime for the electron transport through the system. The corresponding approximations based on Sommerfeld expansion have the form [51]:

$$\begin{aligned}G &= \frac{2e^2}{h}\tau(\mu) \equiv G_0\tau(\mu);\\ S &= \frac{\pi^2k^2T}{3|e|\tau(\mu)}\frac{\partial\tau}{\partial E}\bigg|_{E=\mu} \equiv S_0\frac{\partial\ \ln\ \tau(E)}{\partial E}\bigg|_{E=\mu}.\\ \varkappa_{\mathrm{el}} &= \frac{1}{h}\frac{(\pi kT)^2}{3}\tau(\mu)\left(1-\frac{1}{h}\frac{(\pi kT)^2}{3}\left(\frac{\partial\ \ln\ \tau(E)}{\partial E}\right)^2\bigg|_{E=\mu}\right)\end{aligned} \quad (11)$$

Neglecting phonon contribution into the total thermal conductance $\varkappa$ we may compute $\mathrm{ZT} = \frac{GS^2T}{\varkappa_{\mathrm{el}}}$. Another important characteristic of thermoelectric efficiency is the power factor $\mathrm{PF} = S^2G$.

Coulomb interactions between electrons on the dots cause emergence of a gap in the electron transmission spectrum centered at $E = \tilde{E} \equiv E_0 + \frac{1}{2}U$ [20]. The width of the gap is governed by the charging energy, as shown in figure 2 (left panel). Inside the Coulomb gap the transmission is strongly

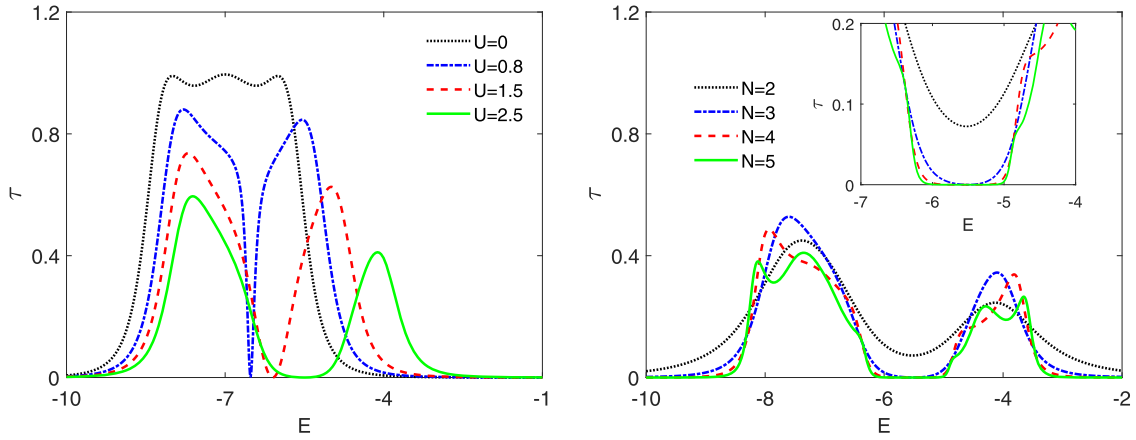

Figure 2. Electron transmission spectra. Curves are plotted assuming $E_0 = -7$, $\Gamma_L = \Gamma_R = 1$ for $N = 3$ (left panel) and $U = 2.5$ (right panel); β is chosen as a unit of energy.

suppressed. When N exceeds a certain number N_0 (which depends on the coupling parameter Γ and takes on greater values in stronger coupled systems), $\tau(\tilde{E})$ becomes zero. This is illustrated in the right panel of figure 2. As shown in the inset, at chosen values of relevant energies $\tau(\tilde{E}) = 0$ for $N > 2$.

Basing on line-shapes of the transmission spectra shown in the inset, we may conjecture that at $N > N_0$ the electron transmission inside the Coulomb gap is proportional to $\left(\frac{E-\tilde{E}}{D}\right)^{2k}$, where D is the width of the gap which depends on the charging energy U and k is a whole positive number which becomes greater when the number of dots increases. Thus Coulomb interactions may produce a specific feature in the spectrum of electron transmission of a sufficiently long chain of QDs, which gets more pronounced as the chain lengthens. The feature is centered at $E = \tilde{E}$ and resembles a 'supernode' appearing in the electron transmission spectra of some chain-like molecules as a result of quantum interference in subunits and causing a significant enhancement of thermoelectric effects [47]. A similar enhancement may occur in multiple QDs wired in series due to the effect of Coulomb interactions provided that the number of included single dots is sufficiently large, as demonstrated below.

Suppose that the chemical potential of electrodes is being varied. When an energy level crosses μ, the transmission gets a maximum and the thermopower changes its sign. The electron transmission and the thermopower dependencies on the position of μ are shown in figure 3. In plotting these curves we did assume that inter-dot coupling is sufficiently strong and the electrodes temperatures ($T = 0.25\beta$) exceeds Kondo temperature, so that the system could remain within the Coulomb blockade regime. First we omit Coulomb interactions between electrons ($U = 0$). Then electron transmission function shows several peaks. The number of peaks coincides with the number of dots in the chain. The electrical conductance G is proportional to τ, thus the conductance oscillates in a similar way, as μ varies. The thermopower also shows saw-toothed oscillations. This is illustrated in the upper panel of figure 3 for $N = 4$. Oscillations of both G and S were first predicted in multiple QDs in parallel configuration [52] and further analyzed in several works [49, 53]. Thermopower oscillations accompanying varying chemical potential of electrodes were observed in single-molecule junctions [54]. Note that in the considered case the oscillations appear regardless of Coulomb interactions between electrons, unlike those discussed in previous works [49, 52, 53].

When electron–electron interactions are included ($U \neq 0$), two peaks located at $\mu = E_0$ and $\mu = E_0 + U$ emerge in the transmission of a single QD, and S changes its sign at these values of μ and at the middle point between these two ($\mu = \tilde{E}$), as expected (see the middle panel). Note that in this case the transmission takes on nonzero value over the whole range between $\mu = E_0$ and $\mu = E_0 + U$. For a chain including four dots ($N = 4$) the Coulomb gap emerges in the electron transmission spectrum, and a quasi-periodicity of τ and S behavior vanishes. When $\tilde{E}$ is located in the vicinity of μ the transmission is suppressed and the thermopower exhibits a giant derivative-like feature originating from the Coulomb gap in the transmission, as displayed in the lower panel of this figure. Such feature does not appear in the case of a single dot sandwiched between the electrodes.

When a gate voltage V_{g0} is applied across the considered transport junction, it shifts the electron transmission spectrum. We may present this shift as $\Delta E = |e|V_g$, where V_g is that portion of the voltage created by the gates which directly falls upon the chain compiled out of QDs. The relationship between the voltages V_{g0} and V_g is a rather complicated one, and we do not explore it here. Nevertheless, we can treat the main characteristics of thermoelectric transport as dependent on V_g. Such dependencies of S, ZT and PF are shown in figures 4 and 5. At fixed U the enhancement of both Seebeck coefficient and ZT occurring due to the presence of the Coulomb gap becomes more pronounced when the number of dots N increases. This is shown in the left panels of figures 4 and 5. The dependence of the thermopower on the charging energy is more complex. The charging energy U determines the Coulomb gap width and affects the position of its center. Accordingly, varying U at a fixed N we shift positions and change widths of the corresponding features emerging in S and ZT versus V_g curves due to the Coulomb gap. At low values of U these features heights are increasing fast as the charging energy enhances but at greater U the increase is slowing down. For the thermopower,

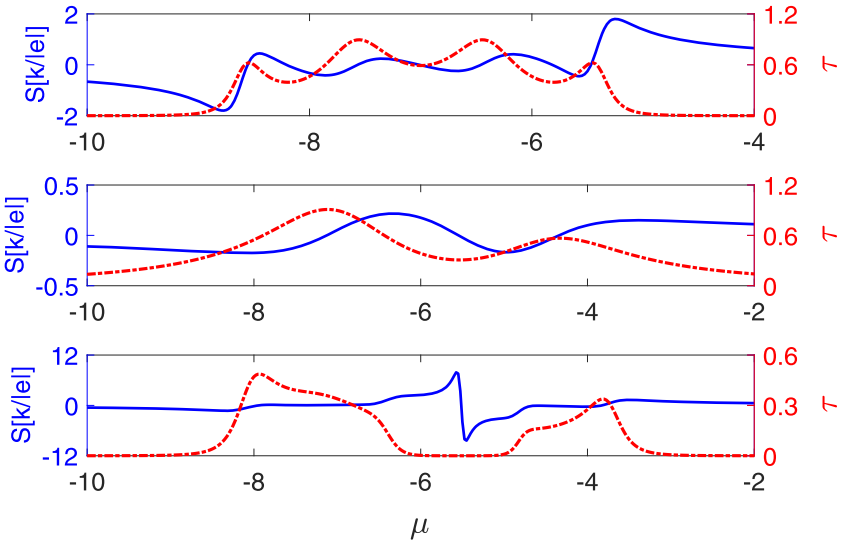

Figure 3. Electron transmission and the corresponding thermopower plotted at $E = \mu$ (μ being the chemical potential of electrodes) as functions of μ for $N = 4$, $U = 0$ (upper panel); for $N = 1$, $U = 2.5$ (middle panel) and for $N = 4$, $U = 2.5$ (lower panel) assuming that $kT = 0.25$, $E_0 = -7$, $\Gamma_L = \Gamma_R = 1$. All energies are measured in the units of β.

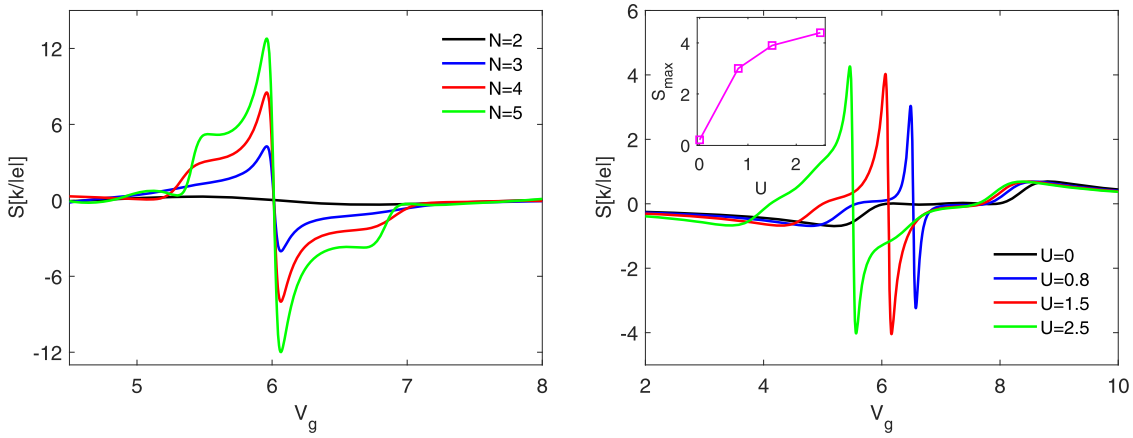

Figure 4. Thermopower S as a function of the voltage V_g plotted for $U = 2.5$ and several values of N (left) and for $N = 3$ and several values of U (right) assuming that $\mu = 0$, $kT = 0.25$, $E_0 = -7$, $\Gamma_L = \Gamma_R = 1$. Here, β is used as the unit of energy and $\beta/|e|$ as the unit of voltage.

this trend is illustrated in the inset to figure 4. We may expect that at sufficiently high U the curve shown there will level off, and the charging energy influence on S and ZT maximum values will cease to exist. This may happen because only a small part of the transmission spectrum around $E = \mu$ determines the values of these characteristics. When μ is placed in the middle of a fairly broad Coulomb gap, $\tau(\mu)$ remains equal to zero over the whole relevant energy range regardless of the specific value of U.

The power factor S^2G is an important characteristic of thermoelectric efficiency along with the figure of merit ZT. To further justify the thermoelectric enhancement one needs to show that PF increases due to the presence of the Coulomb gap in the transmission spectra of long chains made out of QDs. Results displayed in figure 5 are providing for the necessary justification. It is shown that PF reaches a maximum when the gate voltage drags the middle point of the Coulomb gap $E = \tilde{E}$ into a close vicinity of the chemical potential μ (see the left panel). Assuming that U is fixed, the height of this peak significantly increases as N grows. Note that in the case of $N = 1$ (a single dot) and $N = 2$ (a double dot wired in series) where $\tau(\tilde{E}) \neq 0$, the peak heights are much smaller than those corresponding to greater number of dots ensuring a well formed Coulomb gap to appear. The power factor also shows a complex dependence on the charging energy, as illustrated in the right panel of figure 5. One observes that at fixed N peaks associated with the Coulomb gap have maximum height at certain moderate values of the charging energy and are becoming lower as U further increases. Again, this may happen due to the specifics of the transmission spectra around $E = \tilde{E}$, which was discussed above.

When a gate voltage forces a transmission peak situated beyond the Coulomb gap to cross $E = \mu$, a derivative-like feature in S also emerges as shown in the right panel of figure 4. However, magnitudes of these features are much smaller than those related to the Coulomb gap in the transmission spectrum. Therefore one may conclude that intra-dot Coulomb interactions in long chains of QDs (or in long chain-like molecules)

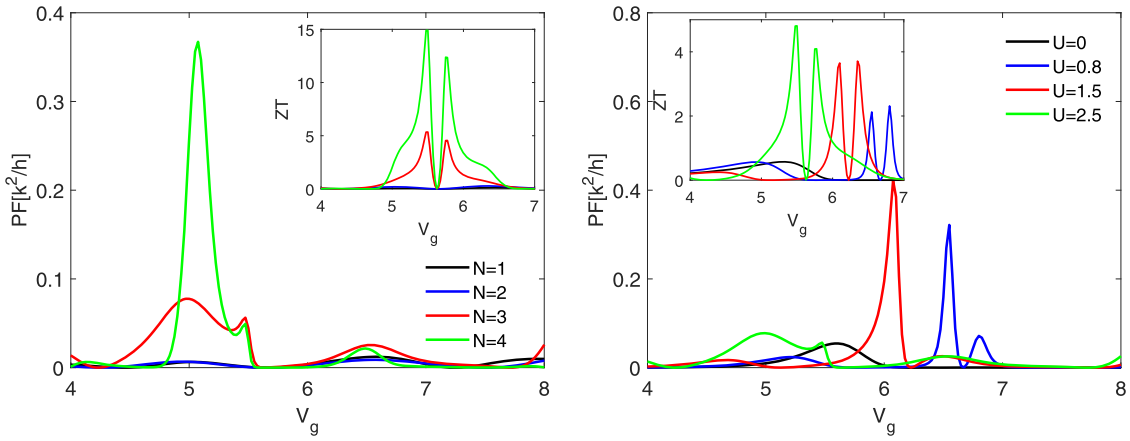

Figure 5. The power factor S^2G as a function of the voltage V_g plotted for $U = 2.5$ and several values of N (left) and for $N = 3$ and several values of the charging energy U (right) assuming that $\mu = 0$, $kT = 0.25$, $\Gamma_L = \Gamma_R = 1$ meV, $E_0 = -7$. Insets show the corresponding dependencies of ZT on V_g. Here, β is used as the unit of energy and $\beta/|e|$ as the unit of voltage.

may give rise to a giant thermoelectric effect and significantly improve the efficiency of heat-to-electric energy conversion in such systems provided that phonon contribution into the thermal conductance is small and $\varkappa \approx \varkappa_{el}$.

4. Conclusion

In the present work we focused on thermoelectric transport through a system consisting of several QDs in a serial configuration placed in between nonmagnetic conducting electrodes. Specifically, we studied the effect of intra-dot Coulomb interactions on Seebeck coefficient, thermoelectric power factor $PF = S^2G$ and thermoelectric figure of merit ZT within the Coulomb blockade regime. Effects of electron–phonon interactions on the electron transport were assumed to be small, and coherent electron tunneling was considered to be a predominating transport mechanism. Transport characteristics were computed using the Green's functions formalism.

Within the adopted tight-binding model, the electron transmission spectra for the considered multiple dot in the absence of electron–electron interactions display sets of peaks symmetrically arranged around the on-dot energy E_0. The number of peaks equals the number of QDs in the considered system. Correspondingly, when the chemical potential is varies the electron conductance G and the thermopower S show a series of oscillations whose number also equals N.

Intra-dot Coulomb interactions cause the emergence of a gap in the transmission spectrum thus bringing qualitative changes into the electron thermoelectric transport. When the number of dots in the chain is sufficiently large, an additional derivative-like feature associated with the Coulomb gap emerges in Seebeck coefficient as well as in PF and ZT at appropriate values of the gate voltage. The features magnitudes strongly exceed all remaining values of these quantities thus indicating a possibility of a giant thermoelectric effect and the improvement of efficiency of energy conversion in the considered transport junctions.

Obtained results resemble those reported in reference [47] where the great enhancement of Seebeck coefficient originated from transmission 'supernodes' appearing in the transmission spectra of some chain-like molecules due to interference effects. In the present case, the interference effects are not important but Coulomb interactions cause the transmission to vanish over a certain energy range thus affecting characteristics of thermoelectric transport in a similar way.

Presented results were obtained omitting effects of electron–phonon interactions on the electron transport. In general, thermal conductance $\varkappa$ differs from the result given by equation (11) and describing the electron contribution $\varkappa_{el}$. It includes an additional phonon term which may noticeably enhance the total $\varkappa$ and thus reduce ZT. However, the phonon contribution into the thermal conductance of multiple QDs may be significantly suppressed by appropriate design of the system, as suggested in several works (see e.g. references [46, 47, 55, 56]). Therefore we believe that the presented results may be useful for further understanding and modeling of thermoelectric transport through multiple QDs and long molecules and for manufacturing nanoscale energy converters.

Acknowledgments

This work was supported by NSF-DMR-PREM 2122102. The author thanks G M Zimbovsky for help with the manuscript preparation.

Data availability statement

Data sharing is not applicable as no new data are created in this study.

ORCID iDs

Natalya A Zimbovskaya https://orcid.org/0000-0002-5419-3675

References

[1] Giazotto F, Heikkilä T T, Luukanen A, Savin A M and Pekola J P 2006 *Rev. Mod. Phys.* **78** 217
[2] Dubi Y and Di Ventra M 2011 *Rev. Mod. Phys.* **83** 131
[3] Sothmann B, Sánchez R and Jordan A N 2015 *Nanotechnology* **26** 032001
[4] Noori M, Sadeghi H and Lambert C J 2017 *Nanoscale* **9** 5299
[5] Reddy P, Jang S-Y, Segalman R A and Majumdar A 2007 *Science* **315** 1568
[6] Malen J A, Doak P, Baheti K, Tilley T D, Segalman R A and Majumdar A 2009 *Nano Lett.* **9** 1164
[7] Widawski J R, Chen W, Vásquez H, Kim T, Breslow R, Hybertsen M S and Venkataraman L 2013 *Nano Lett.* **13** 2889
[8] Pauli F, Viljas J K and Cuevas J C 2008 *Phys. Rev.* B **78** 035315
[9] Finch C M, Garcia-Suarez V M and Lambert C J 2009 *Phys. Rev.* B **79** 033405
[10] Karlström O, Strange M and Solomon G C 2014 *J. Chem. Phys.* **140** 044315
[11] Li R-X, Ni Y, Li H-D, Tian X-L, Yao K-L and Fu H-H 2016 *Physica* B **493** 1
[12] Tsutsui M, Yokota K, Morikawa T and Taniguchi M 2017 *Sci. Rep.* **7** 44276
[13] Leijinse M, Wegewijs M R and Flensgerg K 2010 *Phys. Rev.* B **82** 045412
[14] Craven G T and Nitzan A 2017 *J. Chem. Phys.* **146** 092305
[15] Koch T, Loos J and Fehske H 2014 *Phys. Rev.* B **89** 155133
[16] Galperin M, Nitzan A and Ratner M A 2008 *Mol. Phys.* **106** 397
[17] Simine L, Chen W J and Segal D 2015 *J. Phys. Chem* C **119** 12097
[18] Kruchinin S and Pruschke T 2014 *Phys. Lett.* A **378** 1157
[19] Sowa J K, Mol J A, Briggs G A D and Gauger E M 2017 *Phys. Rev.* B **95** 085423
[20] Trocha P and Barnás J 2012 *Phys. Rev.* B **85** 085408
[21] Wíerbicki M and Swírcowicz R 2011 *Phys. Rev.* B **84** 075410
[22] Khedri A, Meden V and Costi T A 2017 *Phys. Rev.* B **96** 195156
[23] Trocha P and Barnaś J 2017 *Phys. Rev.* B **95** 165439
[24] Estrada Saldaña J C, Vekris A, Steffensen G, Žitko R, Krogstrup P, Paaske J, Grove-Rasmussen K and Nygård J 2018 *Phys. Rev. Lett.* **121** 257701
[25] Abdullah N R, Tang C-S, Manolescu A and Gudmundsson V 2016 *ACS Photonics* **3** 249
[26] Abbas M A A, Al-Badry L F and Al-Khursan A H 2021 *Opt. Quantum Electron.* **53** 421
[27] Wíerbicki M and Swírcowicz R 2010 *Phys. Rev.* B **82** 165334
[28] Szukiewicz B and Wysokinski K I 2015 *Eur. Phys. J.* B **88** 112
[29] Boese D and Fazio R 2011 *Europhys. Lett.* **56** 576
[30] Dubi Y and Di Ventra M 2009 *Phys. Rev.* B **79** 081302
[31] Rejec T, Mravlje J and Ramsak A 2012 *Phys. Rev.* B **85** 085117
[32] Karwacki L and Trocha P 2016 *Phys. Rev.* B **94** 085418
[33] Xu L, Li Z-J, Niu P and Nie Y-H 2016 *Phys. Lett.* A **380** 3553
[34] Zimbovskaya N A 2016 *J. Chem. Phys.* **145** 221101
[35] López R and Sánchez D 2013 *Phys. Rev.* B **88** 045129
[36] Sánchez D and López R 2016 *C. R. Phys.* **17** 1060
[37] Murphy P, Mukerjee S and Moorre J 2008 *Phys. Rev.* B **78** 161406(R)
[38] Kubala B, Konig J and Pecola J 2008 *Phys. Rev. Lett.* **100** 066801
[39] Monteros A L, Uppal G S, McMillan S R, Crisan M and Ţifrea I 2014 *Eur. Phys. J.* B **87** 302
[40] Xu W-P, Zhang Y-Y, Wang Q, Li Z-J and Nie Y-H 2016 *Phys. Lett.* A **380** 958
[41] Siérra M A, Saiz-Bretín M, Domínguez-Adame F and Sánchez D 2016 *Phys. Rev.* B **93** 235452
[42] Zimbovskaya N A 2016 *J. Phys.: Condens. Matter.* **28** 183002
[43] Zimbovskaya N A 2020 *J. Chem. Phys.* **153** 124712
[44] Cheng Y, Li Z, Wei J, Luo H-G and Lin H-Q 2021 *Phys. Lett.* A **415** 127657
[45] Nozaki D, Pastawski H M and Cuniberti G 2010 *New J. Phys.* **12** 063004
[46] Tsaousidou M and Triberis G P 2010 *J. Phys.: Condens. Matter.* **22** 355304
[47] Bergfield J P, Solis M A and Stafford C A 2010 *ACS Nano* **4** 5314
[48] Kuo D M-T and Chang Y-C 2007 *Phys. Rev. Lett.* **99** 086803
[49] Chang Y-C and Kuo D M-T 2008 *Phys. Rev.* B **77** 245412
[50] Datta S 2005 *Quantum Transport: From Atom to Transistor* (Cambridge: Cambridge University Press)
[51] Paulson M and Datta S 2003 *Phys. Rev.* B **67** 241403
[52] Beenakker C W J and Staring A A M 1992 *Phys. Rev.* B **46** 9667
[53] Swíerkowicz R, Wíerbicki M and Barnás J 2010 *Phys. Rev.* B **80** 195409
[54] Morikawa T, Arima A, Tsutsui M and Taniguchi M 2014 *Nanoscale* **6** 8235
[55] Kuo D M-T and Chang Y-C 2010 *Phys. Rev.* B **81** 205321
[56] Yan L, Wang L, Carriguez A R, Lang J, Annadata H V, Antonana M A, Barko E and Nijhuis C A 2018 *Nat. Nanotechnol.* **13** 322–34